Unambiguous Identification of Carbon Location on the N Site in Semi-insulating GaN

Shan Wu,[1] Xuelin Yang,[1,*] Haishan Zhang,[2] Lin Shi,[2] Qing Zhang,[3] Qiuyu Shang,[3] Zeming Qi,[4] Yue Xu,[1] Jie Zhang,[1] Ning Tang,[1] Xinqiang Wang,[1,5] Weikun Ge,[1] Ke Xu,[2] and Bo Shen[1,5,†]

[1]*State Key Laboratory of Artificial Microstructure and Mesoscopic Physics, School of Physics, Peking University, Beijing 100871, People's Republic of China*
[2]*Suzhou Institute of Nano-Tech and Nano-Bionics, Chinese Academy of Sciences, Suzhou 215123, People's Republic of China*
[3]*Department of Materials Science and Engineering, College of Engineering, Peking University, Beijing 100871, People's Republic of China*
[4]*National Synchrotron Radiation Laboratory, University of Science and Technology of China, Hefei 230029, People's Republic of China*
[5]*Collaborative Innovation Center of Quantum Matter, Beijing 100871, People's Republic of China*

(Received 20 May 2018; published 5 October 2018)

Carbon (C) doping is essential for producing semi-insulating GaN for power electronics. However, to date the nature of C doped GaN, especially the lattice site occupation, is not yet well understood. In this work, we clarify the lattice site of C in GaN using polarized Fourier-transform infrared and Raman spectroscopies, in combination with first-principles calculations. Two local vibrational modes (LVMs) at 766 and 774 cm^{-1} in C doped GaN are observed. The 766 cm^{-1} mode is assigned to the nondegenerate A_1 mode vibrating along the $\boldsymbol{c}$ axis, whereas the 774 cm^{-1} mode is ascribed to the doubly degenerate E mode confined in the plane perpendicular to the $\boldsymbol{c}$ axis. The two LVMs are identified to originate from isolated $\mathrm{C_N^-}$ with local C_{3v} symmetry. Experimental data and calculations are in outstanding agreement both for the positions and the intensity ratios of the LVMs. We thus provide unambiguous evidence of the substitutional C atoms occupying the N site with a −1 charge state in GaN and therefore bring essential information to a long-standing controversy.

DOI: 10.1103/PhysRevLett.121.145505

Semiconductors have to be doped with impurities to engineer new and improved properties. For instance, GaN, which represents today an extremely important semiconductor family, has a wide range of modern applications, including light-emitting diodes [1], laser diodes [2], and power electronics [3]. While p-type and n-type GaN for optoelectronic devices are achieved with dopants of Mg and Si, respectively [4,5], semi-insulating GaN, as a core component of power electronic devices, is usually achieved by carbon (C) doping [6]. However, the doping behaviors, especially the lattice site occupation of C in GaN, still remain in debate. As a group IV element, C is amphoteric in GaN, i.e., it may occupy either Ga site to form $\mathrm{C_{Ga}}$ or N site to form $\mathrm{C_N}$, and they can also coexist with each other, individually or forming complexes with other defects [7–12]. However, there is so far no direct experimental evidence for the lattice site of C in GaN, partially due to a lack of effective characterization methods, despite the fact that the identification of the lattice location of Mg in GaN has made great progress recently [13]. As a result, there are lots of controversies about C related defects and their roles in electrical and optical properties. For example, the origin of the semi-insulating characteristic in C doped GaN, being attributed either to the compensation through $\mathrm{C_N}$ acceptor states alone [7,14], or to the self-compensation through interplay between $\mathrm{C_N}$ and $\mathrm{C_{Ga}}$ states, still remains a puzzle [9,15–17]. Understanding those two origins is crucial not only for defect physics but also for reducing the current collapse effect which is the fundamental bottleneck for today's GaN power electronic devices [6,17]. Referring to the optical properties related to C doping, whether the isolated $\mathrm{C_N}$ or $\mathrm{C_N}$-$\mathrm{O_N}$ complex that contributes to the long-standing problem about the origins of the GaN yellow luminescence (YL), has still been a subject of controversy even very recently [10,18]. As such, there remain controversial for the C related defects in GaN although they have been investigated for more than 20 years. All those unsolved problems require an unambiguous identification of the lattice location of C impurity in GaN.

Localized vibrational modes (LVMs) provide detailed insight into the physical properties of light impurities doped in semiconductors. C related LVMs have been reported for a number of cubic semiconductors such as GaAs [19], InAs [20], and InP [21]. However, spectroscopic studies on LVMs of C incorporation in wurtzite GaN have not been explored intensively [22–24]. The main reason is that the wurtzite GaN and the commonly used sapphire substrate exhibit strong Reststrahlen-related band, which obscures many LVMs of dopants in GaN from infrared transmission experiments [25,26]. Some simple assignments of the

 © 2018 American Physical Society

single mode in the range of 770–780 cm^{-1} in C doped GaN in recent literatures [23,24] were still inconclusive, as being a lack of clarification of the symmetry and belonging phonon mode of the LVMs, and fewer number of the LVM modes they observed.

In this Letter, we report an unambiguous evidence of isolated C_N^- in GaN with C_{3v} point group. Polarization-resolved Fourier-transform infrared (FTIR) and Raman spectroscopies reveal two LVMs of C in GaN for the first time. The position and Raman intensity under specific polarizations of the LVMs are all in excellent agreement with the theoretical results. Our data and analysis thus yield a complete and clear picture of the vibrational properties of substitutional C on the N site with −1 charge state in GaN.

The investigated C doped GaN layers were grown on top of AlN/AlGaN transition layers on p-type Si (111) substrates by metal organic chemical vapor deposition (MOCVD). The C incorporation in the GaN layer (∼4 μm) was achieved by intrinsic doping technique and the concentration was determined by secondary ion mass spectrometry (SIMS) analysis. Three GaN samples with C concentrations of 3×10^{16}, 2×10^{18}, and 9×10^{19} cm^{-3} were investigated. The samples were found to be semi-insulating, except the first one exhibiting n-type behavior. FTIR reflection measurements were carried out using a vacuum spectrometer (Bruker IFS-66V) with resolution of 0.25 cm^{-1} on the infrared beamline (BL01B) at the National Synchrotron Radiation Laboratory of China. Raman spectroscopy was performed with a backscattering geometry using a laser with wavelength of 532 nm. First-principles calculations were carried out, as implemented in the PWmat [27,28], in which the electronic interactions are described by the ultra-soft pseudopotential (USPP) [29], and the local-density approximation (LDA) [30] was employed for the exchange-correlation potential. A $4\times4\times2$ supercell with 128 atoms was used for the simulation of the C related defects. All the crystal structures are fully relaxed with the mesh of a $1\times1\times1$ k-point grid, and the force criteria were 0.001 eV $\mathrm{\AA}^{-1}$. We carried out the calculation using the combined dynamic matrix (CDM) method as described in Refs. [31,32] to get the phonon modes and phonon density of states (DOSs) of the defects.

Figure 1(a) shows the nonpolarized FTIR spectra (near normal incident) at 5 K of C doped GaN films with different C concentrations. Besides an absorption peak (reflection dip) of A_1 (LO) mode at 738 cm^{-1}, two new peaks located at ∼769 (denoted as ω_1, and shifted to 768 cm^{-1} at room temperature) and ∼777 cm^{-1} (denoted as ω_2, and shifted to 775 cm^{-1} at room temperature) are resolved from heavily C doped GaN films. With increasing C concentration, the intensities of both peaks increase, suggesting that the two peaks are related to the incorporation of C in GaN and most likely the C related LVMs. Raman spectroscopy is also performed to compensate well with the IR results, as revealed in Fig. 1(b). For the heaviest doped GaN, we can

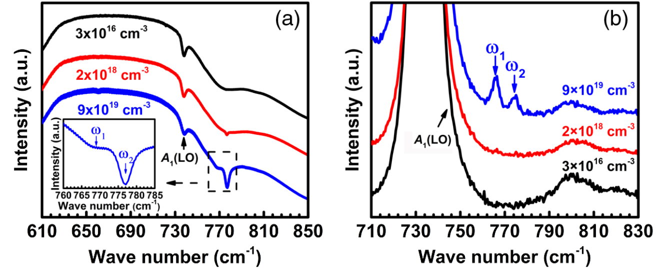

FIG. 1. (a) FTIR reflectance spectra (5 K) of C doped GaN layers with different C concentrations. The inset is the enlarged line showing ω_1 and ω_2. (b) Raman spectra of C doped GaN layers with different C concentrations.

also clearly observe two sharp peaks at 766 and 774 cm^{-1}, which decorated on the high-frequency shoulder of the A_1 (LO). The frequencies of these two distinct peaks observed in the Raman spectra agree well with those observed in the FTIR spectra, so we also denote them as ω_1 and ω_2.

To obtain further information on the symmetry of the LVMs, polarized FTIR spectroscopy is investigated for the heaviest C doped GaN. Figure 2(a) displays the p-polarization spectra at various incident angles φ. In this case, $\mathbf{E}$ can be decomposed to a vector parallel to the $\boldsymbol{c}$ axis and the other one perpendicular to it, both of which vibrate in the incident plane. At near normal incident angle (13°, $\sim\mathbf{E}\perp\boldsymbol{c}$), the spectra reveal only intense ω_2 mode. When increasing φ, the intensity of ω_2 decreases while ω_1 gradually increases. Finally, at the grazing incident angle (83º, $\sim\boldsymbol{E}//\boldsymbol{c}$), the intensity of the two modes is comparable. Figure 2(b) shows the case of the s polarization ($\mathbf{E}\perp\boldsymbol{c}$). We can find that only the sharp ω_2 mode is clearly observed, regardless of angles of incidence φ. Figure 2(c) displays the integral intensity of the two LVMs as well as A_1 (LO) as a function of the polarization angle θ. In order to see more clearly, we choose the case of near normal incident angle for ω_2 as well as A_1 (LO) and the case of grazing incident angle for ω_1. When tuning θ from 0° to 90° and finally to 180°, one can find that ω_2 shows intense absorption with its intensity being independent on θ. Thus, according to Figs. 2(a)–2(c), we could attribute ω_2 to the vibration perpendicular to the $\boldsymbol{c}$ axis with no polarization dependence. For ω_1, it shows strong polarization dependency with the strongest intensity appearing in the p polarization. On the basis of those polarization behaviors, we assign ω_1 to a vibration parallel to the $\boldsymbol{c}$ axis.

Polarization-resolved Raman spectroscopy is also conducted. Figure 3 shows the Raman spectra in $\bar{z}(xx)z$ and $\bar{z}(xy)z$ configurations, as well as nonpolarized configuration. In the nonpolarized configuration, both ω_1 and ω_2 are activated simultaneously. The baseline of the two peaks is subtracted and the ratio of their Raman integral intensity is about 2.2∶1.0. In the $\bar{z}(xx)z$ configuration, ω_1 as well as ω_2 are activated simultaneously, but the intensity of ω_2 is relatively weaker. The ratio is calculated to be about

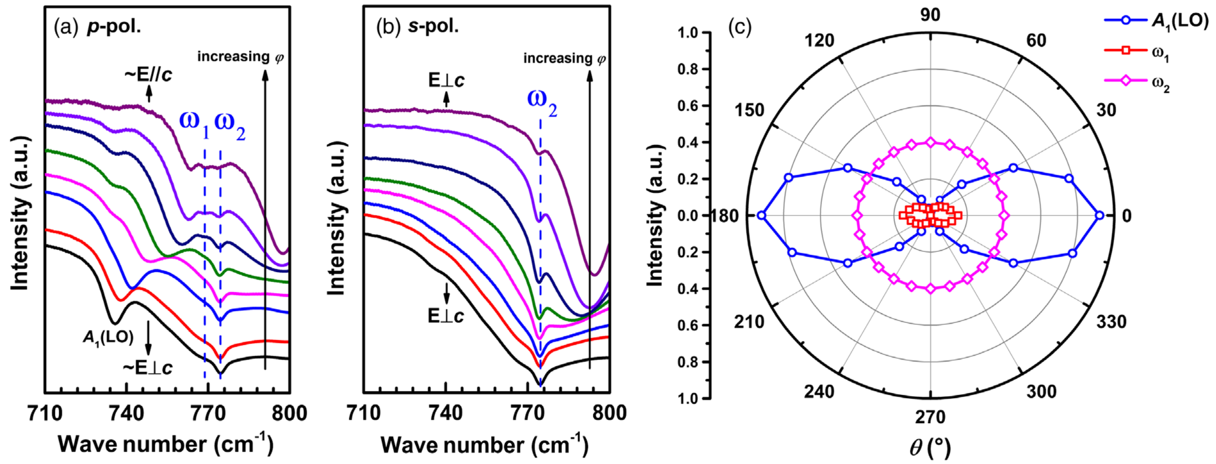

FIG. 2. FTIR reflectance spectra on the heaviest (9×10^{19} cm^{-3}) C doped GaN in the (a) p-polarization, (b) s-polarization configuration with different incident angles φ. (c) Intensity of ω_2 and A_1 (LO) with near normal incident angle as well as ω_1 ($\times 2$) with near grazing incident angle as a function of the polarization angle θ, with 0º denoted to **E** vibrating in the incident plane and 90º vibrating perpendicular to the incident plane.

4.3 : 1.0. However, in the $\bar{z}(xy)z$ configuration, the situation changes drastically and the spectrum shows ω_2 alone. The weak signal of A_1 (LO) is just due to the imperfect polarizer and it should be absent under ideal conditions. Therefore, it can be concluded from the polarized Raman spectra and FTIR spectra that ω_1 vibrates along the $\boldsymbol{c}$ axis with polarization similar to that of A_1 (LO), while ω_2 vibrates perpendicular to the $\boldsymbol{c}$ axis with polarization similar to that of E_2 in the host GaN.

The most likely C related defects in semi-insulating GaN systems are C_N^-, C_{Ga}^+, and $C_N - O_N^0$, considering the formation energies of those defects are relatively low when the Fermi level is close to the middle of the band gap [10,11]. To identify those defects accordingly, the first-principles calculations have been performed. Both the positions and intensity ratios of the local phonons are calculated. For comparison, the calculated and experimental results are summarized together in Table I. We can find that in the calculation, for C_N^-, there are three new local phonons with frequencies of 773 (ν_1), 778 (ν_2), and 781 cm^{-1} (ν_3) located at the high energy end of the bulk phonon DOSs. For C_{Ga}^+, the local phonons are at 837 and 840 cm^{-1}, while for $C_N - O_N^0$ the corresponding peaks are at 757, 777, and 803 cm^{-1}. From the viewpoint of frequency, ω_1 and ω_2 in the FTIR and Raman experiments are close to ν_1-ν_3 from C_N^- within several wave number deviations; thus it has been suggested that the new peaks in the spectra are most likely from C_N^-. In order to shed light

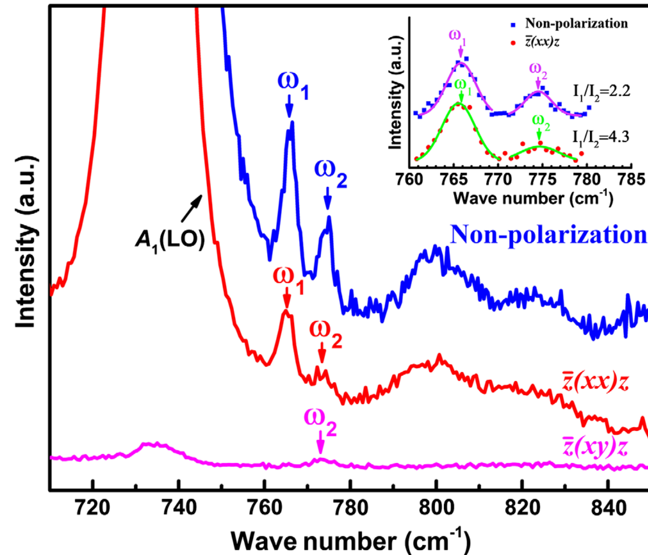

FIG. 3. (a) Room temperature Raman spectra of the heaviest C doped GaN film in the nonpolarized, $\bar{z}(xx)z$ and $\bar{z}(xy)z$ configurations. The inset is the enlarged fitting curves (with baseline subtraction and normalization) of LVMs in the nonpolarized and $\bar{z}(xx)z$ configurations.

TABLE I. Experimental and calculated frequencies (cm^{-1}) as well as the Raman intensity ratios between A_1 and E modes in the C_N^- defect. Frequencies (cm^{-1}) of phonons induced by C_N^0, C_N^+, $C_N - O_N^0$, and C_{Ga}^+ defects are also calculated for comparison.

C related defect		Calculation	Experiment
C_N^-	Frequency/assignment	$773(\nu_1)/A_1$ $778(\nu_2)/E$, $781(\nu_3)/E$	$766(\omega_1)/A_1$ $774(\omega_2)/E$
	Ratio (Nonpol.)	2.3 : 1.0	2.2 : 1.0
	Ratio ($\bar{z}(xx)z$)	4.4 : 1.0	4.3 : 1.0
	Ratio ($\bar{z}(xy)z$)	~0	~0
C_N^0	Frequency	726, 728, 759	⋯
C_N^+	Frequency	703, 715, 720	⋯
$C_N - O_N^0$	Frequency	757, 777, 803	⋯
C_{Ga}^+	Frequency	837, 840	⋯

on the effects of charge state, we also performed calculations for C_N^0 and C_N^+ and the results are given in Table I, too. However, for these phonons calculated, not only the impurity C atom but also its neighbor N atoms vibrate obviously in the phonon modes. They are thus not perfectly spatially localized modes. Furthermore, the frequencies of most of these phonons are far from the values of the LVMs observed in the FTIR and Raman spectra. Although the phonons at 759 cm^{-1} in the C_N^0 and 757 cm^{-1} as well as 777 cm^{-1} in the $C_N - O_N^0$ are also very close to ω_1 or ω_2, further calculated results show that the vibrational direction and the polarized behaviors of those phonons do not agree with any peak in the experiments. Therefore, we can assume that the two lines in the experiments are indeed correlated to the LVMs of isolated C_N with the -1 charge state.

In a supercell with 128 atoms, C atom squeezes itself into the GaN host (C_{3v} point group symmetry) and replaces an N atom as C_N. For the C_N^- defect, after relaxing the system, the C-Ga bond along the $\boldsymbol{c}$ axis is 1.9025 Å (less than N-Ga bond 1.9198 Å), and the other three C-Ga bonds are all 1.8955 Å (less than N-Ga bond 1.9201 Å). Then we find that the C_N^- defect displays a local symmetry of C_{3v}. That is also confirmed by the Raman tensor obtained from the calculation results (not shown here). Furthermore, the schematic diagrams of the energy levels with the fundamental dipole transitions for a C_N^- defect with C_{3v} symmetry are depicted in Fig. 4. Based on group theory, defects with C_{3v} symmetry give two infrared and Raman active LVMs (A_1 and E) [33]. The A_1 mode is nondegenerate and the vibration orientated along the $\boldsymbol{c}$ axis, whereas the E mode is doubly degenerate and the corresponding phonons are orthogonal with its motion confined in the plane perpendicular to the $\boldsymbol{c}$ axis. It is shown in the calculation that ν_1 orientates along the $\boldsymbol{c}$ axis and the other two are orthogonal and confined in the c plane. We thus confidently suggest that ν_1 belongs to A_1 mode, while ν_2 and ν_3 are doubly degenerate belonging to E mode with the same frequency.

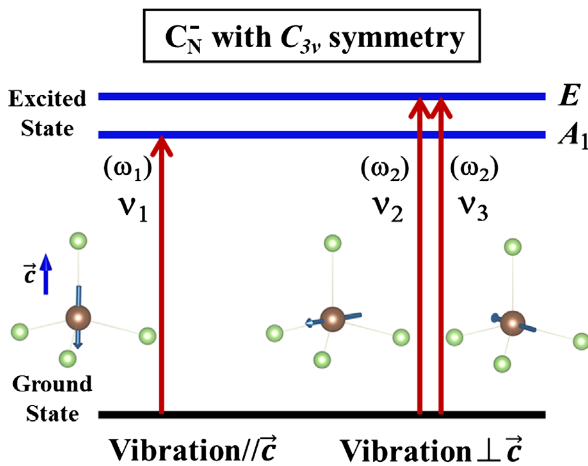

FIG. 4. The schematic energy level diagrams and fundamental dipole transitions in a C_N^- center with C_{3v} symmetry. The calculated vibrational directions of C atom are also depicted. The larger brown spheres represent C atoms, while the smaller green spheres represent Ga atoms.

We now turn to the experimental and calculated results about the intensity ratios as shown in Table I. In the nonpolarized configuration, the intensity ratio of the out-of-plane (ν_1) and in-plane phonons (ν_2 and ν_3) is calculated to be about 2.3∶1.0, when we sum up the Raman intensity of ν_2 and ν_3. This value agrees very well with the experimental result of 2.2∶1.0. In this case, ν_1 (A_1 mode), ν_2 (E mode), and ν_3 (E mode) are activated simultaneously. In the $\bar{z}(xx)z$ configuration, the Raman ratio changes to 4.4∶1.0, which also agrees well with the experimental result of 4.3∶1.0. This is because only ν_1 and ν_2 could be activated under this condition. While in the $\bar{z}(xy)z$ configuration, the Raman intensity of ν_1 is about 0, consistent with the fact that ω_1 is absent in the Raman spectrum. This is because only ν_3 is active and the other two modes are silent. All the results presented above clearly demonstrate that the observed ω_1 (corresponding to ν_1 in calculation) and ω_2 (corresponding to ν_2 and ν_3 in calculation) refer to A_1 and E modes of point group C_{3v}, respectively. Therefore, the consistent results between the spectroscopic experiments and the calculations do unambiguously confirm that the two modes are the LVMs of substitutional C atoms at N lattice sites, i.e., isolated C_N with -1 charge state. We should emphasize that the two LVMs have never been observed together before.

The LVMs of C_{Ga} and C_N-O_N are not observed even in the heaviest C doped samples; we thus believe that their concentrations are low even though their existence cannot be ruled out completely. Other C atomic configurations such as the interstitial site (C_I) and/or their complexes with C_N (i.e., C_I-C_N) have not been discussed and require further investigations. However, in the case of semi-insulating GaN, their concentrations are expected to be low due to the higher formation energies [11]. Therefore, we confirm that the majority of C occupy the N sites in semi-insulating GaN. Finally, we comment on the charge states of C_N. In the heaviest C doped GaN, the O and Si concentrations are 10^{15}–10^{16} cm^{-3}, as determined by SIMS. The low values imply that there should exist other donors that associate with C_N in the -1 charge state. We therefore suggest that the donor may be N vacancies (V_N). We also find some evidence that their concentration increases with C incorporation into GaN from Raman spectra. Especially, recent theoretical work demonstrated that V_N^+ is the main donor and the concentration is comparable to that of C_N^- in GaN when the concentrations of O, Si, and H are low [12]. That is in good agreement with our experimental results. We should claim that the growth details [34] and doping approaches should be taken into account when analyzing the lattice sites and charge states of C in GaN. For example,

intrinsic and extrinsic C doping may affect the lattice sites of C in GaN and that would be an interesting topic. Nevertheless, the present results contribute significantly to in-depth understanding of the C related defects and their role in electrical as well as optical properties in GaN. We believe that the spectroscopic studies, combined with the first-principles calculations, would be a universal approach for identification of the lattice sites of C in other compound semiconductors such as AlN, BN, ZnO, and Ga_2O_3.

In summary, from the viewpoint of symmetry, the present study provides direct observation of two LVMs of isolated C_N in GaN by performing FTIR and Raman scattering experiments. We find that the LVM at 766 cm^{-1} (ω_1) orientated along the ***c*** axis corresponds to the nondegenerate A_1 mode, while the LVM at 774 cm^{-1} (ω_2) confined in *c* plane corresponds to the doubly degenerate *E* mode. The present spectroscopic work offers an unambiguous evidence that C is predominantly located on the N sublattice in GaN with −1 charge state, and keeps with C_{3v} symmetry. That conclusion is in excellent agreement with the calculation results. We believe that the present work will be proved to be even more useful in interpreting the long-standing problem about the role of C in GaN.

This work was supported by the National Key Research and Development Program of China (Grants No. 2016YFB0400104, No. 2017YFB0402900, and No. 2016YFB0400201) and the National Natural Science Foundation of China (Grants No. 61574004, No. 61521004, No. 11634002, No. U1601210, and No. 61522401). We are grateful for the professional services offered by the Platforms of Characterization and Test at SINANO, and Supercomputing Center, CNIC, CAS.

[*]xlyang@pku.edu.cn
[†]bshen@pku.edu.cn

[1] S. Nakamura, T. Mukai, and M. Senoh, Appl. Phys. Lett. **64**, 1687 (1994).
[2] F. A. Ponce and D. P. Bour, Nature (London) **386**, 351 (1997).
[3] J. Simon, V. Protasenko, C. X. Lian, H. L. Xing, and D. Jena, Science **327**, 60 (2010).
[4] F. A. Reboredo and S. T. Pantelides, Phys. Rev. Lett. **82**, 1887 (1999).
[5] P. Boguslawski and J. Bernholc, Phys. Rev. B **56**, 9496 (1997).
[6] M. J. Uren, J. Moreke, and M. Kuball, IEEE Trans. Electron Devices **59**, 3327 (2012).
[7] J. L. Lyons, A. Janotti, and C. G. Van de Walle, Phys. Rev. B **89**, 035204 (2014).
[8] M. A. Reshchikov, D. O. Demchenko, A. Usikov, H. Helava, and Y. Makarov, Phys. Rev. B **90**, 235203 (2014).
[9] A. F. Wright, J. Appl. Phys. **92**, 2575 (2002).
[10] D. O. Demchenko, I. C. Diallo, and M. A. Reshchikov, Phys. Rev. Lett. **110**, 087404 (2013).
[11] M. Matsubara and E. Bellotti, J. Appl. Phys. **121**, 195701 (2017).
[12] M. Matsubara and E. Bellotti, J. Appl. Phys. **121**, 195702 (2017).
[13] U. Wahl *et al.*, Phys. Rev. Lett. **118**, 095501 (2017).
[14] J. L. Lyons, A. Janotti, and C. G. Vande Walle, Appl. Phys. Lett. **97**, 152108 (2010).
[15] M. Huber, I. Daumiller, A. Andreev, M. Silvestri, L. Knuuttila, A. Lundskog, M. Wahl, M. Kopnarski, and A. Bonanni, J. Appl. Phys. **119**, 125701 (2016).
[16] B. Rackauskas, M. J. Uren, S. Stoffels, M. Zhao, S. Decoutere, and M. Kuball, IEEE Trans. Electron Devices **65**, 1838 (2018).
[17] G. Verzellesi, L. Morassi, G. Meneghesso, M. Meneghini, E. Zanoni, G. Pozzovivo, S. Lavanga, T. Detzel, O. Haberlen, and G. Curatola, IEEE Electron Device Lett. **35**, 443 (2014).
[18] S. G. Christenson, W. Y. Xie, Y. Y. Sun, and S. B. Zhang, J. Appl. Phys. **118**, 135708 (2015).
[19] J. Wagner, R. C. Newman, B. R. Davidson, S. P. Westwater, T. J. Bullough, T. B. Joyce, C. D. Latham, R. Jones, and S. Oberg, Phys. Rev. Lett. **78**, 74 (1997).
[20] S. Najmi, M. X. Chen, A. Yang, M. Steger, M. L. W. Thewalt, and S. P. Watkins, Phys. Rev. B **74**, 113202 (2006).
[21] R. C. Newman, B. R. Davidson, J. Wagner, M. J. L. Sangster, and R. S. Leigh, Phys. Rev. B **63**, 205307 (2001).
[22] G. Kaczmarczyk, A. Kaschner, A. Hoffmann, and C. Thomsen, Phys. Rev. B **61**, 5353 (2000).
[23] S. Ito, H. Kobayashi, K. Araki, K. Suzuki, N. Sawaki, K. Yamashita, Y. Honda, and H. Amano, J. Cryst. Growth **414**, 56 (2015).
[24] M. F. Cerqueira, L. G. Vieira, A. Alves, R. Correia, M. Huber, A. Andreev, A. Bonanni, and M. I. Vasilevskiy, J. Phys. D **50**, 365103 (2017).
[25] J. Y. Yang, G. J. Brown, M. Dutta, and M. A. Stroscio, J. Appl. Phys. **98**, 043517 (2005).
[26] J. Ibanez, S. Hernandez, E. Alarcon-Llado, R. Cusco, L. Artus, S. V. Novikov, C. T. Foxon, and E. Calleja, J. Appl. Phys. **104**, 033544 (2008).
[27] W. L. Jia, Z. Y. Cao, L. Wang, J. Y. Fu, X. B. Chi, W. G. Gao, and L. W. Wang, Comput. Phys. Commun. **184**, 9 (2013).
[28] W. L. Jia, J. Y. Fu, Z. Y. Cao, L. Wang, X. B. Chi, W. G. Gao, and L. W. Wang, J. Comput. Phys. **251**, 102 (2013).
[29] D. Vanderbilt, Phys. Rev. B **41**, 7892 (1990).
[30] J. P. Perdew and A. Zunger, Phys. Rev. B **23**, 5048 (1981).
[31] L. Shi and L. W. Wang, Phys. Rev. Lett. **109**, 245501 (2012).
[32] H. S. Zhang, L. Shi, X. B. Yang, Y. J. Zhao, K. Xu, and L. W. Wang, Adv. Opt. Mater. **5**, 1700404 (2017).
[33] D. T. Hon, W. L. Faust, W. G. Spitzer, and P. F. Williams, Phys. Rev. Lett. **25**, 1184 (1970).
[34] Despite the fact that C_N is the predominant lattice site for C in GaN, our ongoing experiments reveal that C_{Ga} does exist with concentration being about 2 orders of magnitude lower than that of C_N in the heaviest C doped GaN samples. In particular, we find that the apparent concentration of C_{Ga} depends on the postgrowth annealing temperature. See Y. Xu *et al.* (to be published).